



Published in final edited form as:

Nature. 2010 December 23; 468(7327): 1095–1099. doi:10.1038/nature09587.

## Subtypes of medulloblastoma have distinct developmental origins

Paul Gibson<sup>1</sup>, Yiai Tong<sup>1</sup>, Giles Robinson<sup>1,2</sup>, Margaret C. Thompson<sup>9</sup>, D. Spencer Currie<sup>1</sup>, Christopher Eden<sup>1</sup>, Tanya A. Kranenburg<sup>1</sup>, Twala Hogg<sup>1</sup>, Helen Poppleton<sup>1</sup>, Julie Martin<sup>1</sup>, David Finkelstein<sup>3</sup>, Stanley Pounds<sup>4</sup>, Aaron Weiss<sup>10</sup>, Zoltan Patay<sup>5</sup>, Matthew Scoggins<sup>5</sup>, Robert Ogg<sup>5</sup>, Yanxin Pei<sup>11</sup>, Zeng-Jie Yang<sup>11</sup>, Sonja Brun<sup>11</sup>, Youngsoo Lee<sup>6</sup>, Frederique Zindy<sup>6</sup>, Janet C. Lindsey<sup>12</sup>, Makoto M. Taketo<sup>13</sup>, Frederick A. Boop<sup>7</sup>, Robert A. Sanford<sup>7</sup>, Amar Gajjar<sup>2</sup>, Steven C. Clifford<sup>12</sup>, Martine F. Roussel<sup>6</sup>, Peter J. McKinnon<sup>6</sup>, David H. Gutmann<sup>14</sup>, David W. Ellison<sup>8</sup>, Robert Wechsler-Reya<sup>11</sup>, and Richard J. Gilbertson<sup>1,2</sup>

<sup>1</sup> Dept. of Developmental Neurobiology, St Jude Children's Research Hospital, 262 Danny Thomas Place, Memphis, TN, 38105, USA <sup>2</sup> Dept. of Oncology, St Jude Children's Research Hospital, 262 Danny Thomas Place, Memphis, TN, 38105, USA <sup>3</sup> Hartwell Center for Bioinformatics and Biotechnology, St Jude Children's Research Hospital, 262 Danny Thomas Place, Memphis, TN, 38105, USA <sup>4</sup> Dept. of Biostatistics, St Jude Children's Research Hospital, 262 Danny Thomas Place, Memphis, TN, 38105, USA <sup>5</sup> Dept. of Radiological Sciences, St Jude Children's Research Hospital, 262 Danny Thomas Place, Memphis, TN, 38105, USA <sup>6</sup> Dept. of Genetics and Tumor Cell Biology, St Jude Children's Research Hospital, 262 Danny Thomas Place, Memphis, TN, 38105, USA <sup>7</sup> Dept. of Surgery, St Jude Children's Research Hospital, 262 Danny Thomas Place, Memphis, TN, 38105, USA <sup>8</sup> Dept. of Pathology, St Jude Children's Research Hospital, 262 Danny Thomas Place, Memphis, TN, 38105, USA <sup>9</sup> Department of Pediatric Hematology/Oncology, The Cleveland Clinic, 9500 Euclid Ave/S20, Cleveland, OH 44195, USA <sup>10</sup> Robert Wood Johnson Medical School, 195 Little Albany Street, New Brunswick, NJ 08903 <sup>11</sup> Dept. of Pharmacology and Cancer Biology, Duke University Medical Center, Durham, NC 27710, USA <sup>12</sup> Northern Institute for Cancer Research, Newcastle University, Newcastle upon Tyne, Newcastle upon Tyne, NE2 4HH, England <sup>13</sup> Graduate School of Medicine, Kyoto University, Yoshida-Konoé-cho, Sakyo, Kyoto 606-8501, Japan <sup>14</sup> Department of Neurology, Washington University School of Medicine, St. Louis, Missouri 63110, USA

Users may view, print, copy, download and text and data- mine the content in such documents, for the purposes of academic research, subject always to the full Conditions of use: [http://www.nature.com/authors/editorial\\_policies/license.html#terms](http://www.nature.com/authors/editorial_policies/license.html#terms)

Correspondence should be addressed to RJG: Richard.Gilbertson@stjude.org.

**Author contributions.** R.J.G. conceived the research and planned experiments. P.G., also planned and conducted the great majority of the experiments. Y.T., G.R., D.S.C., M.C.T., T.H., H.P., J.M., J.C.L., Y.L., F.Z., C.E., S.C.C., M.F.R., P.J.M., and R.W-R., conducted experiments. D.F., and S.P., provided bioinformatic expertise. A.G., F.A.B., and R.A.S., provided clinical advice and tumor samples. D.H.G., provided the *Blbp-Cre* mouse and data. M.M.T., provided the *Ctnnb1<sup>lox(ex3)/lox(ex3)</sup>* mouse. Z.P., and R.O., reviewed and analyzed the human MRI scans. D.W.E., provided pathology review. All authors contributed to the writing of the manuscript.

### Competing interests.

None.

Supplementary Information  
Supplemental Information is available online.

## Abstract

Medulloblastoma encompasses a collection of clinically and molecularly diverse tumor subtypes that together comprise the most common malignant childhood brain tumor<sup>1–4</sup>. These tumors are thought to arise within the cerebellum, with approximately 25% originating from granule neuron precursor cells (GNPCs) following aberrant activation of the Sonic Hedgehog pathway (hereafter, SHH-subtype)<sup>3–8</sup>. The pathological processes that drive heterogeneity among the other medulloblastoma subtypes are not known, hindering the development of much needed new therapies. Here, we provide evidence that a discrete subtype of medulloblastoma that contains activating mutations in the WNT pathway effector *CTNNB1* (hereafter, WNT-subtype)<sup>1,3,4</sup>, arises outside the cerebellum from cells of the dorsal brainstem. We found that genes marking human WNT-subtype medulloblastomas are more frequently expressed in the lower rhombic lip (LRL) and embryonic dorsal brainstem than in the upper rhombic lip (URL) and developing cerebellum. Magnetic resonance imaging (MRI) and intra-operative reports showed that human WNT-subtype tumors infiltrate the dorsal brainstem, while SHH-subtype tumors are located within the cerebellar hemispheres. Activating mutations in *Ctnnb1* had little impact on progenitor cell populations in the cerebellum, but caused the abnormal accumulation of cells on the embryonic dorsal brainstem that included aberrantly proliferating *Zic1*<sup>+</sup> precursor cells. These lesions persisted in all mutant adult mice and in 15% of cases in which *Tp53* was concurrently deleted, progressed to form medulloblastomas that recapitulated the anatomy and gene expression profiles of human WNT-subtype medulloblastoma. We provide the first evidence that subtypes of medulloblastoma have distinct cellular origins. Our data provide an explanation for the marked molecular and clinical differences between SHH and WNT-subtype medulloblastomas and have profound implications for future research and treatment of this important childhood cancer.

---

SHH-subtype medulloblastoma is characterized by aberrant SHH signaling that is often driven by inactivating mutations in *PTCH1*<sup>3,4</sup>. These medulloblastomas tend to arise in very young children, display a ‘large cell-anaplastic’ or ‘desmoplastic’ histology and have a relatively poor prognosis<sup>2–4</sup>. WNT-subtype medulloblastomas are strikingly different. Arising in much older children, these highly curable tumors have ‘classic’ morphology and activating mutations in *CTNNB1*<sup>1–4</sup>. Mouse models have shown that SHH-subtype medulloblastomas arise from committed GNPCs of the cerebellum<sup>7,8</sup> and enabled the development of new therapies that suppress the oncogenic SHH-signal<sup>9,10</sup>. It has been suggested that the other medulloblastoma subtypes might have a different cellular origin<sup>5,11,12</sup>, but little is known about their biology and there are no mouse models of these tumors.

Recently, we showed that subtypes of the brain tumor ependymoma arise from discrete populations of neural progenitor cells with which they share similar gene expression profiles<sup>13</sup>. Therefore, to determine if medulloblastoma subtypes also arise from discrete cell populations, we first used four online gene expression databases to chart the regional expression of 110 genes that mark human SHH or WNT-subtype medulloblastomas<sup>3</sup>. Twenty-four WNT-subtype and 25 SHH-subtype medulloblastoma signature genes are contained within ‘Brain Explorer 2’ that generates 3-dimensional gene expression maps across the mouse brain ([www.brain-map.org](http://www.brain-map.org), Supplemental Methods, Supplemental Dataset 1). As expected<sup>14</sup>, these data revealed the URL at embryonic day (E) 11.5 and the E15.5

cerebellum to be the most common sites of SHH-subtype signature gene expression (Figure 1a,b and Supplemental Dataset 1). In contrast, WNT-subtype medulloblastoma signature genes were predominantly expressed within the E11.5 LRL (rhombomeres [r]2-r8) and the E15.5 dorsal brainstem. Expression of an additional 61 medulloblastoma signature genes, reported by three other online databases, confirmed this differential pattern (Supplemental Figure 1, Supplemental Table 1). These data suggest that SHH and WNT-subtype medulloblastomas arise from distinct regions of the hindbrain and identify the dorsal brainstem as a potential source of WNT-subtype tumors.

If SHH and WNT-subtype medulloblastomas have different origins then we reasoned that these tumors should demonstrate anatomical differences at diagnosis. Remarkably, all validated WNT-subtype medulloblastomas examined (n=6/6, Supplemental Figure 2) were located within the IV ventricle and infiltrated the dorsal surface of the brainstem; while all SHH-subtype tumors (n=6/6) were distributed away from the brainstem within the cerebellar hemispheres (Figure 1c,d, Supplemental Figure 3, exact Mann-Whitney  $P < 0.005$ ). Five of the six WNT-subtype, but no SHH-subtype tumors, were adherent to the dorsal brainstem at surgery (Fisher's Exact Test,  $P < 0.005$ ). Thus, WNT-subtype medulloblastomas are anatomically distinct from SHH-tumors and are intimately related to the IV ventricle and dorsal brainstem.

We noted various cell types surrounding the IV ventricle that could give rise to WNT-subtype medulloblastomas, including dorsal brainstem progenitors of cochlear, mossy fiber (MF) and climbing fiber (CF) neurons (Figure 1a,b; Supplemental Figure 4)<sup>15</sup>. But it remained possible that cerebellar ventricular zone (VZ) radial glia<sup>12,16</sup> or GNPCs generate WNT-subtype medulloblastomas. To identify hindbrain cells that are susceptible to transformation by *Ctnnb1*, we generated mice carrying a cre-dependent mutant allele of *Ctnnb1* (*Ctnnb1<sup>lox(ex3)</sup>*)<sup>17</sup> and the *Blbp-Cre* transgene<sup>18</sup>. *Blbp-Cre* induces efficient recombination in progenitor cell populations across the hindbrain including the cerebellar VZ, GNPCs of the external germinal layer (EGL) and Olig3<sup>+</sup> progenitor cells in the LRL<sup>19</sup> (Supplemental Figure 5). We also generated *Blbp-Cre<sup>+/-</sup>; Ctnnb1<sup>+lox(ex3)</sup>* (hereon, *Ctnnb1*-mutant) mice that were homozygous for a cre-dependent mutant allele of *Tp53* (*Tp53<sup>flx</sup>*)<sup>20</sup> since loss of this tumor suppressor accelerates medulloblastoma formation in *Ptch1<sup>+/-</sup>* mice<sup>21</sup>. As expected, *Ctnnb1*-mutant embryos expressed mutant nuclear-Ctnnb1 in all hindbrain germinal zones, regardless of *Tp53* status (Supplemental Figures 5k and 6). Surprisingly, mutation of *Ctnnb1* did not affect significantly the proliferation or apoptosis of VZ cells or GNPCs in the cerebellum (Figure 2a and Supplemental Figure 7).

Since GNPCs generate SHH-subtype medulloblastomas<sup>7,8</sup> we sought additional evidence that these cells are not impacted by mutant Ctnnb1. First, we generated *Atoh1-Cre<sup>+/-</sup>; Ctnnb1<sup>+lox(ex3)</sup>* mice since *Atoh1-Cre* drives efficient recombination in GNPCs, generating medulloblastomas in conditional *Ptch1* mice (see Supplemental Figure 8a-j and Ref. 7). We also used the *Atoh1* enhancer element present in the *Atoh1-Cre* allele, to drive expression of a constitutively active Ctnnb1-green fluorescence fusion protein in GNPCs (*Atoh1-Ctnnb1<sup>N90GFP</sup>*, Supplemental Figure 8k-o)<sup>22</sup>. Neither *Atoh1-Cre<sup>+/-</sup>; Ctnnb1<sup>+lox(ex3)</sup>* nor *Atoh1-Ctnnb1<sup>N90GFP</sup>* mice (>20 mice examined each) developed hyperplasia or masses within the URL or EGL. Concordantly, aberrant Ctnnb1 signaling did not impact the

proliferation of GNPCs *ex vivo* (Supplemental Figure 8p). Thus, in contrast to aberrant Shh signaling, mutant *Ctnnb1* does not appear to disrupt cell cycle or differentiation control in GNPCs.

In stark contrast to the cerebellum, by E16.5 all *Ctnnb1*-mutant mice developed aberrant cell collections in the dorsal brainstem that persisted into adulthood (exact Mann-Whitney  $P < 0.005$ , Figure 2a–f). These cells were marked by *Olig3* and *Pax6* suggesting they may be derived from progenitor cells within the LRL<sup>19,23</sup> (Figure 2d,e). This abnormality was independent of *Tp53* status and did not involve the floor plate that is not targeted by *Blbp-Cre* (Supplemental Figure 9). Progenitors within the embryonic dorsal brainstem proliferate to produce daughter cells that express specific marker proteins and follow complex migration streams to their respective nuclei in the developing brainstem (Supplemental Figure 4)<sup>15</sup>. We observed no significant differences in the overall proliferation (Ki-67 labeling), apoptosis (TUNEL labeling) or cell cycle duration (5-bromo-2-deoxyuridine pulse-chase) of progenitors in the dorsal brainstem of *Ctnnb1*-mutant versus control mice (Figure 2c, data not shown). However, a significant fraction of proliferating cells within *Ctnnb1*-mutant dorsal brainstems expressed *Zic1* (37%  $Zic1^+/Ki67^+ = 122/322$ ; Figure 2c,f–h). This expression is aberrant since *Zic1* normally marks postmitotic MF neuron precursors as they exit the dorsal brainstem to form nuclei in the ventral brainstem<sup>23,24</sup> (Figure 2g). Thus, mutant *Ctnnb1* might stall the dorso-ventral migration of brainstem neuron precursors, resulting in aberrant dorsal cell collections<sup>25</sup>. To test this, we used *in utero* GFP-electroporation to track the fate of embryonic dorsal brainstem precursors (Figure 2i–q; Supplemental Figures 10–11). GFP-labeled *Zic1*<sup>+</sup> MF neuron precursors underwent normal migration from the dorsal brainstem to the PGN and other brainstem nuclei in control mice (Figure 2k–n; Supplemental Figure 11). In contrast, mutation of *Ctnnb1* markedly reduced the numbers of precursors transiting from the dorsal brainstem to the PGN (Figure 2o–q; exact Mann-Whitney,  $P < 0.05$ ). Together, these data demonstrate that mutant *Ctnnb1* disrupts the normal differentiation and migration of progenitor cells on the dorsal brainstem, resulting in the accumulation of aberrant cell collections. These cells may include stalled MF neuron precursors, but further work is required to determine their precise lineage.

Aberrant cell collections in the dorsal brainstem of *Ctnnb1*-mutant mice are reminiscent of the EGL hyperplasia that precedes formation of SHH-subtype medulloblastoma in the cerebellum of *Ptch1* deficient mice<sup>26</sup>. Therefore, we aged *Ctnnb1*-mutant mice harboring *Tp53*<sup>+/+</sup>, *Tp53*<sup>+/*flx*</sup> or *Tp53*<sup>*flx/flx*</sup> alleles to test if WNT-subtype medulloblastomas might arise from the dorsal brainstem ( $n > 54$  mice per genotype). Aberrant cell collections persisted throughout adulthood on the dorsal brainstem of all *Ctnnb1*-mutant ; *Tp53*<sup>+/+</sup> mice but these animals did not develop medulloblastoma or tumors in any part of the hindbrain (median follow up 365 days). In contrast, 2 of 10 *Ctnnb1*-mutant ; *Tp53*<sup>*flx/flx*</sup> mice aged <6 months harbored asymptomatic tumors that were confined to the dorsal brainstem (Supplemental Figure 12). When aged for longer periods, 15% ( $n = 8/55$ ) of *Ctnnb1*-mutant ; *Tp53*<sup>*flx/flx*</sup> and 4% ( $n = 2/54$ ) *Ctnnb1*-mutant ; *Tp53*<sup>+/*flx*</sup> mice developed ‘classic’ medulloblastomas that were *Zic1*<sup>+</sup> and contained populations of nuclear-*Ctnnb1*<sup>+</sup>/*Olig3*<sup>+</sup> cells (median follow up 290 and 287 days, respectively; Figure 3a–d). These mouse medulloblastomas displayed an immunoprofile similar to human WNT-subtype tumors and were invariably connected with

the brainstem (Figure 3d–e; Supplemental Figure 13). In contrast, mouse models of human SHH-subtype medulloblastoma<sup>21, 27, 28</sup> are nuclear-*Ctnnb1* negative, arise within the cerebellum and do not invade the brainstem (Figure 3d,e). Together, these data support the hypothesis that progenitor cells within the dorsal brainstem are susceptible to transformation by concurrent mutation in *Ctnnb1* and *Tp53*, resulting in the formation of tumors that mimic the anatomical features of human WNT-subtype medulloblastoma. Deletion of *Tp53* is presumably required to permit key second mutations during transformation of the LRL in *Ctnnb1*-mutant mice. Notably, we have observed two cases of *TP53*-mutant human WNT-subtype medulloblastoma, suggesting this gene also suppresses these tumors in humans (Supplemental Figure 14).

To test further the fidelity of *Ctnnb1*-mutant mouse medulloblastoma as a model of human WNT-subtype disease, we compared the tumor transcriptomes in the two species using an algorithm we have developed for cross-species genomic comparisons<sup>13</sup>. Remarkably, the transcriptome (n=11,049 orthologs) of *Ctnnb1*-mutant ; *Tp53*<sup>flx/flx</sup> medulloblastomas matched only human WNT-subtype medulloblastoma and the cells of the embryonic dorsal brainstem (both permuted  $P < 0.05$ ), validating it as a model of this human tumor subtype and further pinpointing the brainstem as the source of WNT-subtype medulloblastomas (Figure 4a,b). Finally, since human WNT-subtype medulloblastomas selectively delete chromosome 6 (Ref. <sup>3</sup>), we looked in *Ctnnb1*-mutant mouse medulloblastomas to see if syntenic regions of this chromosome are deleted (Figure 4c). DNA microarray analysis identified a single common deletion of mouse chromosome 17 3.2 cM/human 6q25.3 in tumors in the two species. This locus encodes a single gene, *TULP4*, that is a distant member of the tubby-gene family implicated in regulating neuronal cell apoptosis<sup>29</sup>. Thus, *Ctnnb1*-mutant ; *Tp53*<sup>flx/flx</sup> mouse medulloblastomas accurately model the molecular characteristics of human WNT-subtype tumors and pinpoint *TULP4* as a novel candidate suppressor gene of these tumors. By demonstrating that subtypes of medulloblastoma have distinct cellular origins our data should significantly accelerate the hunt for curative treatments of these diseases which must now account for the different developmental origins of these tumors.

## Methods Summary

### MRI analysis

MRI images of patients were spatially normalized into a standard stereotaxic space for quantitative comparison of tumor location (SPM5; [www.fil.ion.ucl.ac.uk/spm](http://www.fil.ion.ucl.ac.uk/spm)). Radiologists masked to patient subtype determined the 3-dimensional location of the tumor or surgical cavity relative to predefined anatomical landmarks.

### Expression mapping

The expression of mouse orthologs of key signature genes of human WNT and SHH-subtype medulloblastoma (Supplemental Dataset 1 and Supplemental Table) were mapped in the developing mouse hindbrain using four publically accessible datasets (see Supplemental Methods).

## Mouse studies

*Blbp-Cre*, *Ctnnb1<sup>lox(ex3)/lox(ex3)</sup>*, *Atoh1-Cre* and *Tp53<sup>flx/flx</sup>* mice were bred to generate appropriate genotypes and subject to clinical surveillance for signs of tumor development. *RosaYFP* and *RosaLacZ* reporter strains traced the lineage of Cre-recombined cells. Mouse tumors comprised 85% tumor cells. *Atoh1-Ctnnb1<sup>N90</sup>* transgenic mice were generated by pro-nuclear injection. *In utero* electroporation and cell tracking were performed by anesthetizing pregnant mice of the appropriate genotype. The uterus was externalized and the dorsal brainstem of E12.5 embryos electroporated with *CMV-eGFP* plasmid DNA. GNPCs for culture studies were isolated from postnatal day 7 *Atoh1-GFP* transgenic mice.  $2 \times 10^5$  GFP<sup>+</sup> cells/well were cultured in poly-D-lysine-coated 96-well plates and challenged with mutant-*Ctnnb1-GFP*, control *GFP* virus, Wnt1 protein (50ng/ml) or Shh supernatant (3ug/ml) prior to pulsing with [methyl-3H]thymidine and scintillation counting.

## Histology, mRNA and DNA microarray profiling

Immunohistochemistry was performed using routine techniques and primary antibodies of the appropriate tissues as described (Supplemental Methods). Cells undergoing apoptosis were detected with the Apoptag kit (Millipore, S7100). mRNA expression (GEO accession number GSE24628) and DNA copy number profiles (available at <http://stjuderesearch.org/site/authors/gilbertson>) were generated from mouse and human tissues using appropriate microarray platforms as detailed (Supplemental Methods). Reverse transcriptase Real Time-PCR analysis and gene re-sequencing of human medulloblastomas were performed as described previously<sup>3</sup>. mRNA expression and DNA microarray profiles of human and mouse medulloblastomas were integrated using established and novel bioinformatic and statistical approaches.

## Supplementary Material

Refer to Web version on PubMed Central for supplementary material.

## Acknowledgments

R.J.G. holds the Howard C. Schott Research Chair from the Malia's Cord Foundation, and is supported by grants from the National Institutes of Health (R01CA129541, P01CA96832 and P30CA021765), the Collaborative Ependymoma Research Network (CERN) and by the American Lebanese Syrian Associated Charities (ALSAC). We are grateful to Anjen Chenn, Jane Johnson and Carmen Birchmeier for their generous gifts of reagents and the staff of the Hartwell Center for Bioinformatics and Biotechnology and ARC at St Jude Children's Research Hospital for technical assistance.

## References

1. Ellison DW, et al. beta-Catenin status predicts a favorable outcome in childhood medulloblastoma: the United Kingdom Children's Cancer Study Group Brain Tumour Committee. *J Clin Oncol.* 2005; 23:7951–7957. [PubMed: 16258095]
2. Gajjar A, et al. Risk-adapted craniospinal radiotherapy followed by high-dose chemotherapy and stem-cell rescue in children with newly diagnosed medulloblastoma (St Jude Medulloblastoma-96): long-term results from a prospective, multicentre trial. *Lancet Oncol.* 2006; 7:813–820. [PubMed: 17012043]
3. Thompson MC, et al. Genomics identifies medulloblastoma subgroups that are enriched for specific genetic alterations. *J Clin Oncol.* 2006; 24:1924–1931. Epub 2006 Mar 19. [PubMed: 16567768]

4. Kool M, et al. Integrated genomics identifies five medulloblastoma subtypes with distinct genetic profiles, pathway signatures and clinicopathological features. *PLoS One*. 2008; 3:e3088. [PubMed: 18769486]
5. Gilbertson RJ, Ellison DW. The Origins of Medulloblastoma Subtypes. *Annu Rev Pathol*. 2008; 3:341–365. [PubMed: 18039127]
6. Goodrich LV, Milenkovic L, Higgins KM, Scott MP. Altered neural cell fates and medulloblastoma in mouse patched mutants. *Science*. 1997; 277:1109–1113. [PubMed: 9262482]
7. Schuller U, et al. Acquisition of granule neuron precursor identity is a critical determinant of progenitor cell competence to form Shh-induced medulloblastoma. *Cancer Cell*. 2008; 14:123–134. [PubMed: 18691547]
8. Yang ZJ, et al. Medulloblastoma can be initiated by deletion of Patched in lineage-restricted progenitors or stem cells. *Cancer Cell*. 2008; 14:135–145. [PubMed: 18691548]
9. Romer JT, et al. Suppression of the Shh pathway using a small molecule inhibitor eliminates medulloblastoma in Ptc1(+/-)p53(-/-) mice. *Cancer Cell*. 2004; 6:229–240. [PubMed: 15380514]
10. Rudin CM, et al. Treatment of Medulloblastoma with Hedgehog Pathway Inhibitor GDC-0449. *N Engl J Med*. 2009; 2:2.
11. Louis, D.; Ohgaki, H.; Wiestler, O.; Cavenee, W., editors. World Health Organization Classification of Tumours of the Central Nervous System. IARC; Lyon: 2007.
12. Huang X, et al. Transventricular delivery of Sonic hedgehog is essential to cerebellar ventricular zone development. *Proc Natl Acad Sci U S A*. 2010; 107:8422–8427. Epub 2010 Apr 8416. [PubMed: 20400693]
13. Johnson RA, et al. Cross-species genomics matches driver mutations and cell compartments to model ependymoma. *Nature*. 2010; 466:632–636. [PubMed: 20639864]
14. Lee Y, et al. A molecular fingerprint for medulloblastoma. *Cancer Res*. 2003; 63:5428–5437. [PubMed: 14500378]
15. Ray RS, Dymecki SM. Rautenlippe Redux -- toward a unified view of the precerebellar rhombic lip. *Curr Opin Cell Biol*. 2009; 21:741–747. [PubMed: 19883998]
16. Morales D, Hatten ME. Molecular markers of neuronal progenitors in the embryonic cerebellar anlage. *J Neurosci*. 2006; 26:12226–12236. [PubMed: 17122047]
17. Harada N, et al. Intestinal polyposis in mice with a dominant stable mutation of the beta-catenin gene. *Embo J*. 1999; 18:5931–5942. [PubMed: 10545105]
18. Hegedus B, et al. Neurofibromatosis-1 Regulates Neuronal and Glial Cell Differentiation from Neuroglial Progenitors In Vivo by Both cAMP- and Ras-Dependent Mechanisms. *Cell Stem Cell*. 2007; 1:443–457. [PubMed: 18371380]
19. Storm R, et al. The bHLH transcription factor Olig3 marks the dorsal neuroepithelium of the hindbrain and is essential for the development of brainstem nuclei. *Development*. 2009; 136:295–305. Epub 2008 Dec 2015. [PubMed: 19088088]
20. Jonkers J, et al. Synergistic tumor suppressor activity of BRCA2 and p53 in a conditional mouse model for breast cancer. *Nat Genet*. 2001; 29:418–425. [PubMed: 11694875]
21. Wetmore C, Eberhart DE, Curran T. Loss of p53 but not ARF accelerates medulloblastoma in mice heterozygous for patched. *Cancer Res*. 2001; 61:513–516. [PubMed: 11212243]
22. Chenn A, Walsh CA. Regulation of cerebral cortical size by control of cell cycle exit in neural precursors. *Science*. 2002; 297:365–369. [PubMed: 12130776]
23. Landsberg RL, et al. Hindbrain rhombic lip is comprised of discrete progenitor cell populations allocated by Pax6. *Neuron*. 2005; 48:933–947. [PubMed: 16364898]
24. DiPietrantonio HJ, Dymecki SM. Zic1 levels regulate mossy fiber neuron position and axon laterality choice in the ventral brain stem. *Neuroscience*. 2009; 162:560–573.10.1016/j.neuroscience.2009.02.082 [PubMed: 19303920]
25. Farago AF, Awatramani RB, Dymecki SM. Assembly of the brainstem cochlear nuclear complex is revealed by intersectional and subtractive genetic fate maps. *Neuron*. 2006; 50:205–218. [PubMed: 16630833]

26. Oliver TG, et al. Loss of patched and disruption of granule cell development in a pre-neoplastic stage of medulloblastoma. *Development*. 2005; 132:2425–2439. Epub 2005 Apr 2420. [PubMed: 15843415]
27. Uziel T, et al. The tumor suppressors Ink4c and p53 collaborate independently with Patched to suppress medulloblastoma formation. *Genes Dev*. 2005; 19:2656–2667. Epub 2005 Oct 2631. [PubMed: 16260494]
28. Frappart PO, et al. Recurrent genomic alterations characterize medulloblastoma arising from DNA double-strand break repair deficiency. *Proc Natl Acad Sci U S A*. 2009; 106:1880–1885. [PubMed: 19164512]
29. Ikeda A, Ikeda S, Gridley T, Nishina PM, Naggert JK. Neural tube defects and neuroepithelial cell death in Tulp3 knockout mice. *Hum Mol Genet*. 2001; 10:1325–1334. [PubMed: 11406614]

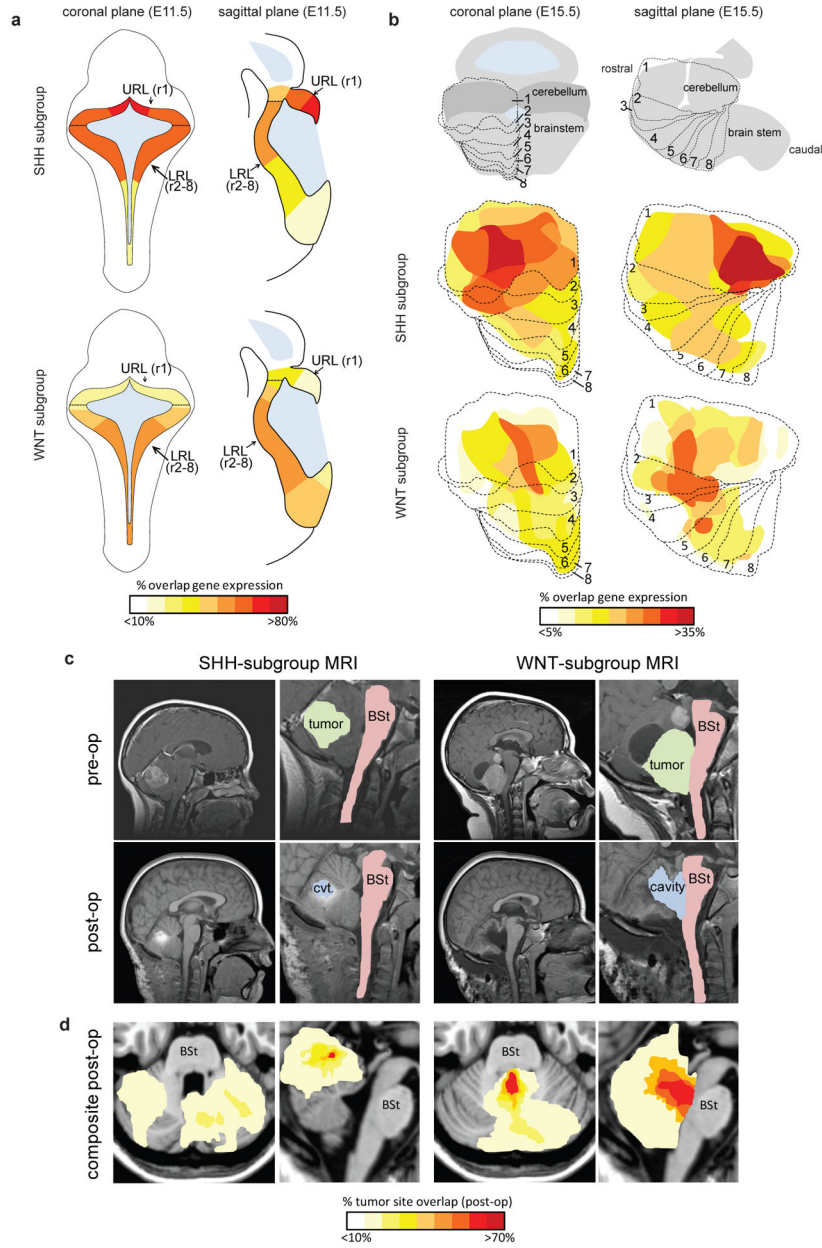


**Figure 1. WNT and SHH-subtypes of medulloblastoma are anatomically distinct**  
**(a)** Expression distribution in **(a)** E11.5 and **(b)** E15.5 mouse hindbrain of orthologs that distinguish human WNT and SHH-subtype medulloblastoma (Supplemental Dataset 1). Cartoons in **(b)** denote the position of rhombomeres relative to the cerebellum and brainstem. **(c)** Top=pre and bottom=post-operative MRI scans of exemplary SHH and WNT-subtype medulloblastomas. Right panels show close up views of left. Brainstem (BSt), post-operative tumor cavity (cvt.). **(d)** Frequency and site of post-operative surgical cavities of SHH (n=6) and WNT (n=6)-subtype medulloblastomas. Axial (left) and sagittal (right) views are shown.



at E12.5. (q) Mean  $\pm$  SD of LRL:PGN GFP-fluorescence in whole hindbrains of three *Blbp-Cre ; Ctnnb1<sup>+/+</sup>* and five *Blbp-Cre ; Ctnnb1<sup>+lox(Ex3)</sup>* mice (graphs, \* 0.05, \*\* 0.005, Exact Mann-Whitney P).

Author Manuscript

Author Manuscript

Author Manuscript

Author Manuscript

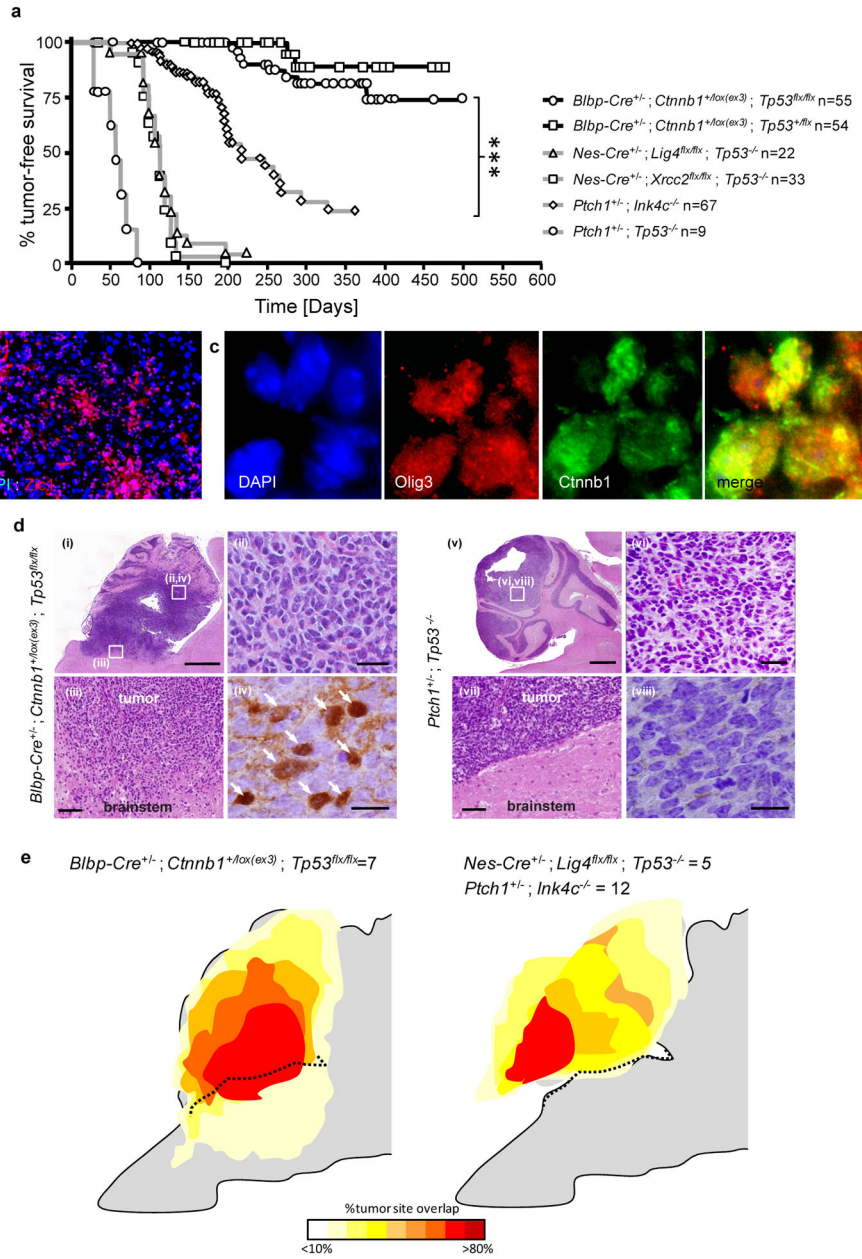


**Figure 3. Mutant-*Ctnnb1* and SHH-subtype mouse medulloblastomas are anatomically distinct** (a) Tumor free survival of SHH-subtype medulloblastoma mouse models (*Nes-Cre<sup>+/+</sup>; Lig4<sup>flx/flx</sup>; Tp53<sup>-/-</sup>*, *Nes-Cre<sup>+/+</sup>; Xrcc2<sup>flx/flx</sup>; Tp53<sup>-/-</sup>*, *Ptch1<sup>+/-</sup>; Ink4c<sup>-/-</sup>*, *Ptch1<sup>+/+</sup>; Tp53<sup>-/-</sup>* data from Refs.<sup>14, 27, 28</sup>) and *Ctnnb1*-mutant; *Tp53<sup>flx/flx</sup>* and *Ctnnb1*-mutant; *Tp53<sup>+/flx</sup>* mice. \*\*\*=Log Rank  $P < 0.0001$ . Immunofluorescence of (b) Zic1 and (c) Olig3 and Ctnnb1 expression in a *Ctnnb1*-mutant; *Tp53<sup>flx/flx</sup>* medulloblastoma. (d) Hematoxylin and eosin stained low (i, v; scale=800  $\mu$ m) and high (ii, vi; scale=25  $\mu$ m) power views of mouse medulloblastomas and tumor-brainstem interface (iii, vii; scale bar=50 $\mu$ m). *Ctnnb1* immunostaining (iv, viii; scale=10  $\mu$ m, arrows indicate nuclear immunoreactivity). Boxes

indicate location of high power views. **(e)** Frequency and anatomical site of mouse medulloblastomas.

Author Manuscript

Author Manuscript

Author Manuscript

Author Manuscript

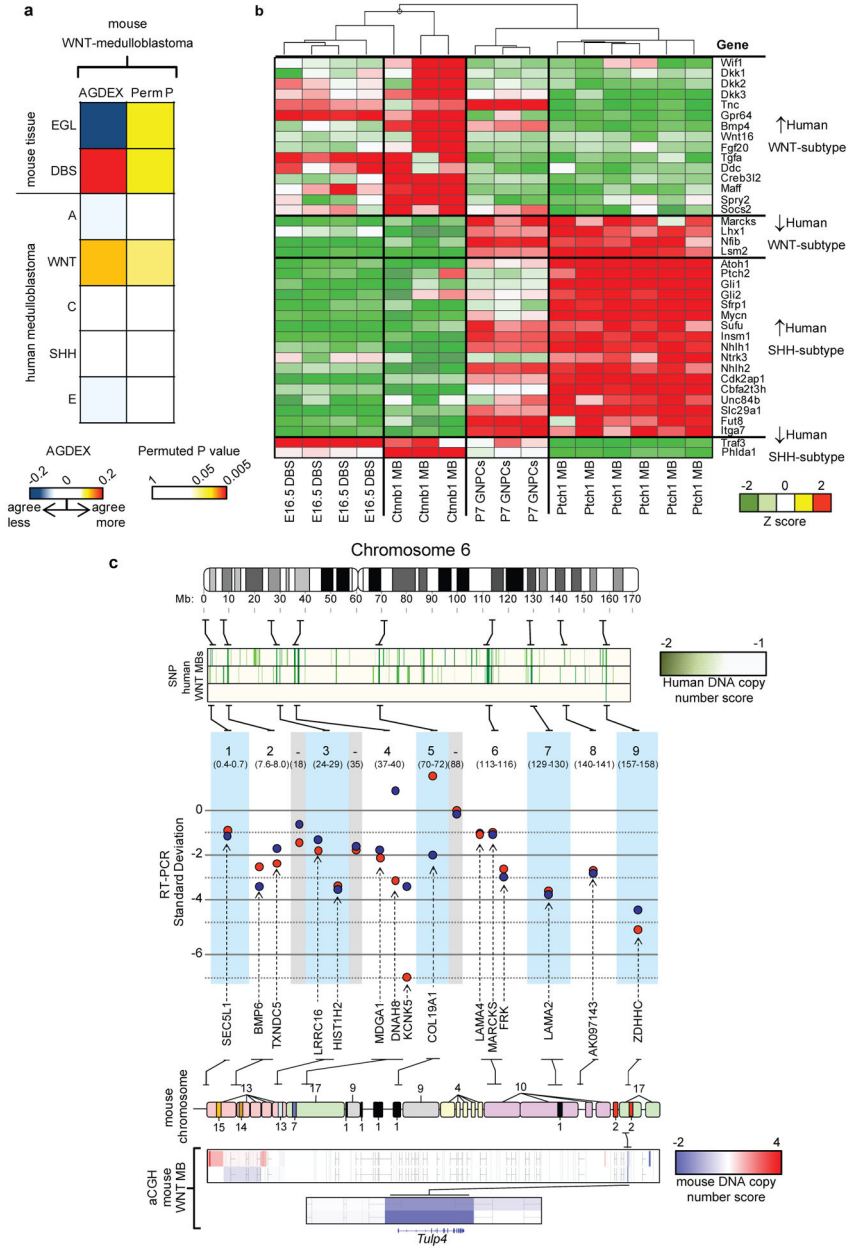


**Figure 4. Mutant-*Ctnnb1* mouse medulloblastomas recapitulate the molecular characteristics of human WNT-subtype disease**

**(a)** AGDEX comparison of *Ctnnb1*-mutant ; *Tp53<sup>flx/flx</sup>* mouse medulloblastoma, and mouse EGL, E16.5 dorsal brainstem (DBS) and human medulloblastoma subgroups. **(b)** Unsupervised clustering of human WNT and SHH-subtype medulloblastoma signature ortholog expression in E16.5 DBS, *Ctnnb1*-mutant ; *Tp53<sup>flx/flx</sup>* mouse medulloblastoma (*Ctnnb1* MB), P7 GNPCs and *Ptch1<sup>+/-</sup>*; *Tp53<sup>-/-</sup>* medulloblastoma (*Ptch1* MB). **(c)** Top-bottom: Nine SNP-inferred homozygous deletions in three human WNT-subtype medulloblastomas. Real-Time PCR validation of deletions in the human tumors (SD below the mean diploid copy-number). Mouse chromosomal regions syntenic for human

chromosome 6. ArrayCGH-inferred copy number in *Ctnnb1*-mutant ; *Tp53<sup>flx/flx</sup>* mouse medulloblastomas identifies common syntenic deletion of *TULP4*.

Author Manuscript

Author Manuscript

Author Manuscript

Author Manuscript